Analysis of Three-Dimensional Potential Flow Around a Ship Hull

Akin Ecer,* Joseph Eichers,† and Theodore Bratanow‡
University of Wisconsin, Milwaukee, Wis.

The method of singularities is applied for the solution of three-dimensional potential flow around arbitrarily shaped bodies. The three-dimensional bodies are represented by systems of singular functions with singularities placed inside the body. An optimization procedure was applied to determine the optimal locations of the singular functions. A rigorous treatment of the problem is presented to establish the validity of the mathematical formulation and the optimization procedure. The method developed here can be applied for analyzing flow around obstacles for which the singularities at the boundaries could not be treated efficiently using presently used techniques. Presented are computational considerations and numerical results showing the velocity distribution around a regularly shaped obstacle and for the bow of an icebreaker.

Introduction

DURING recent years there have been various applications of numerical methods for solution of potential flow problems around arbitrarily shaped bodies.[1-5] Many of these methods have been essentially based on Prager's concept[6] of representing the surface of a three-dimensional body in a flow by a surface distribution of vorticity. Such a vorticity field is approximated at a series of discrete points on the body. Hess and Smith[1,2] have demonstrated the applicability of surface distributions of singularities to the calculation of potential flows around ship hulls and aircraft fuselage-wing combinations. This method has produced interesting numerical results. The procedure given here was developed during an investigation of potential flow around an icebreaker ship.

A considerable portion of the resistance encountered by a moving ice-breaker is due to motion of the broken ice pieces depending on the flow characteristics in the bow region. The influence of the geometric configuration of the bow is complex, and produces several near singularities in the flow. In addition to the consideration of the bow shape, nowadays it is desirable to include the effects of pitching motion of the ship, and sometimes to include even the effect of a bubbler system on the flow patterns. Inclusion of such features in an analysis requires an elaborate and accurate discretized representation of the hull geometry. Difficulties of such a nature can hinder the application of previously developed methods, particularly from the standpoint of computational efficiency.

In the following, details of the mathematical analysis of the potential flow are discussed. Following the method of von Karman,[7] the three-dimensional body is represented by a system of singular functions with singularities placed inside the body. However, compared to previous analyses, an optimum configuration of such functions was sought with the intent to increase the efficiency of the method. The presentation of the mathematical derivation of the analysis is essential for understanding both the method and its advantages. Numerical results were obtained which show the velocity distributions for a regularly shaped obstacle, a sphere, and for an irregularly shaped body, the bow of the USSC Mackinaw, an icebreaker. Computational considerations related to the numerical procedure are discussed. This method is capable of treating any kind of singularities, and it is also efficient in terms of the number of equations to be solved compared to accuracy obtained.

Received July 18, 1974; revision received December 23, 1974. This research was supported by the National Science Foundation under Grant GK-35779 and by NASA under Grant NGR-50-007-001.

Index category: Marine Hydrodynamics, Vessel and Control Surface.

*Associate Professor, Department of Mechanics. Member AIAA.

†Student; presently Project Engineer, Aqua-Chem Company, Milwaukee, Wis. Member AIAA.

‡Professor, Department of Mechanics, Member AIAA.

Mathematical Formulation

The solution of three-dimensional potential flow requires the solution of Laplace's equation

$$\nabla^2 \Phi = 0 \tag{1}$$

where Φ is the velocity potential related to the velocity vector v by

$$v = \nabla \Phi \tag{2}$$

By applying the method of singularities Φ can be represented by a series of singular functions in space. For example, the potential function due to a simple source in a fluid at rest at infinity is

$$\phi = -\frac{m}{r} \tag{3}$$

where r is the distance between any point in the flow and the source, and m represents the strength of the source. ϕ is a singular function with singularity at $r=0$. Similar expressions can be derived for a doublet and for a source or doublet distributions on a curve in three-dimensional space. Using the singular functions one can represent the solution of Φ by

$$\Phi = \sum_{i=1}^{\infty} \phi_i(\delta_i, x_i, y_i, z_i) + \Phi_\infty \tag{4}$$

where δ_i is the magnitude of the source and x_i, y_i, and z_i describe the position of the source. Φ_∞ is the velocity potential of the undisturbed flow without the obstacle.

Since the mathematical problem to be solved is the analysis of flow around the solid obstacle, if all the singular functions in Eq. (4) are placed inside the solid obstacle, then Φ does not include any singularity for the flow region around the body. Every function ϕ_i satisfies Laplace's equation, Eq. (1), automatically. The variables x_i, y_i, and z_i are unknown. Also, as r goes to infinity every ϕ_i goes to zero. Under these conditions, the only requirement left to be satisfied for ϕ to be a solution is to satisfy the boundary conditions on the obstacle surface as

$$\frac{\partial \Phi}{\partial n} = 0 \tag{5}$$

where n represents the normal direction.

At this point one can attempt to find an approximate solution $\tilde{\Phi}$ for Φ by considering only a finite number of terms in Eq. (4),

$$\tilde{\Phi} = \sum_{i=1}^{n} \phi_i(\delta_i, x_i, y_i, z_i) + \Phi_\infty \tag{6}$$

This approximate solution again satisfies Eq. (1) and the boundary conditions at the freestream. It is necessary then to determine a set of functions $\phi_i, i=1, n$ which will satisfy Eq. (5).

An error function θ, defined by

$$\theta = \int_{S'} \left(\frac{\partial \Phi}{\partial n} - \frac{\partial \tilde{\Phi}}{\partial n} \right)^2 dS' \tag{7}$$

is selected because it approaches zero as $\tilde{\Phi}$ converges to Φ and is positive definite. Determining the optimum arrangement of the singularities in this manner helps making the overall analysis tractable from computational and economical standpoint. This function corresponds to a least square approximation of the error function; $\partial\Phi/\partial n$ in Eq. (7) is a known function. The problem then reduces to determining ϕ_i, $i=1$, n which will minimize the error function θ in Eq. (7). At this point, the function θ is discretized by dividing the surface of the obstacle S' into m discrete elements as shown in Fig. 1. $\partial\Phi/\partial n$ is a known function for each element and m is larger than n. As a first approximation, it was assumed that $\partial\Phi/\partial n$ was a constant for each element and was calculated at the centroid of each triangle. The procedure permits the use of higher order variation of $\partial\Phi/\partial n$ over each element by defining more sophisticated surface elements. The discretized form of θ in Eq. (7) can be written as

$$\tilde{\theta} = (A\delta - S)^t D (A\delta - S) \tag{8}$$

when δ is the vector representing the magnitude of the singular functions. A is a (mxn) rectangular matrix, assembled for a given configuration of n singular functions in space and defines the induced velocities at m points on the obstacle surface due to n sources. D in this case is a diagonal matrix, consisting of the areas of the surface elements. S is a vector representing the values of the known function $\partial\Phi/\partial n$ at each of the boundary points.

By minimizing $\tilde{\theta}$ with respect to δ_i,

$$A^t DA\delta = A^t DS \tag{9}$$

or

$$\delta = (A^t DA)^{-1} A^t DS \tag{10}$$

and after substituting Eq. (10) into Eq. (8), $\tilde{\theta}$ can be written as

$$\tilde{\theta} = S^t DS - S^t DA (A^t DA)^{-1} A^t DS \tag{11}$$

The exact solution corresponds to $\tilde{\theta}=0$. However, instead of searching for $\tilde{\theta}=0$, we can introduce another function Γ where

$$\Gamma = \frac{S^t DA (A^t DA)^{-1} A^t DS}{S^t DS} \tag{12}$$

As $\tilde{\theta}$ goes to zero, Γ will converge to one. The optimum solution will then correspond to matrix A, which for Γ assumes a value closest to one. In Appendix A, it is shown that

$$\Gamma < 1 \text{ when } m > n \tag{13}$$

$$\Gamma = 1 \text{ when } m = n \tag{14}$$

A direct optimization of Γ, however, requires excessive computational effort since at each step of the optimization a (nxn) matrix has to be inverted. Therefore, instead of using Γ as a function to be optimized, another function Γ^* was chosen such that

$$\Gamma^* < \Gamma < 1 \tag{15}$$

Then as Γ^* goes to one, Γ, will also converge to one, if we choose Γ^* as follows:

$$\Gamma^* = \frac{(\tilde{S}^t \tilde{A} \tilde{A}^t \tilde{S})^2}{[\tilde{S}^t \tilde{A} (\tilde{A}^t \tilde{A}) \tilde{A}^t \tilde{S}] [\tilde{S}^t \tilde{S}]} \tag{16}$$

The validity of Eq. (15) for the Γ^* in Eq. (16) is shown in Appendix A.

The Computational Procedure

The numerical solution of the problem consists of determining the series of singular functions $(\phi_i, i=1,n)$ in Eq. (4), where the magnitude of each of these functions is determined from Eq. (12), and they are geometrically placed in a manner to maximize Γ^* in Eq. (16). The use of Eq. (16) instead of Eq. (12) is advantageous since one does not have to invert $(A^t A)$ every time this matrix is modified.

The numerical procedure can be summarized as follows: Initially n singular functions with n singularities are placed inside the solid obstacle at points (x_i, y_i, z_i) which are arbitrary at the outset of the computational procedure. The obstacle surface is represented by m elements as shown in Fig. 1. Matrix A is assembled and Γ^* is calculated. Then matrix A is modified by changing the positions of the singularities in space. After an optimal Γ^* is determined, the magnitudes of the singular functions are calculated from Eq. (10). The mesh on the obstacle surface is designed in a way to allow for increase of accuracy by using smaller elements around certain critical points. The initial placement of the singular functions is critical since depending on the type of singular functions used, the induced velocity decays rapidly away from the singularity.

Discussion of Results

Numerical results for two examples are presented to demonstrate the applicability of the numerical procedure. The initial case, the analysis of potential flow around a sphere, served for testing the procedure. The exact solution in this case is due to a single doublet, placed at the center of the sphere. For this particular example, increasing number of doublets were placed in an axisymmetric fashion around the center of the sphere, as shown in Fig. 2. Variation of normal velocities on the surface of the sphere are shown in Figs. 3 and 4. The accuracy of the solution in terms of positions and numbers of doublets is shown in Figs. 5 and 6. From these results one can observe the importance of the number and locations of the singular functions employed in the analysis, since both number and location of doublets (see Table 1) control the accuracy. It is possible that a good initial location can give ac-

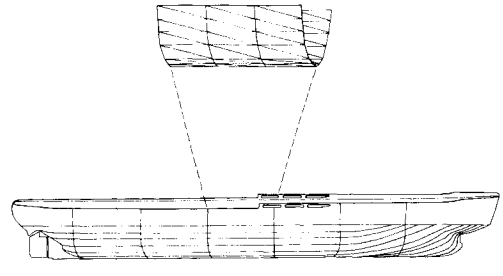

Fig. 1 Schematic of hull gridwork details for the potential flow analysis.

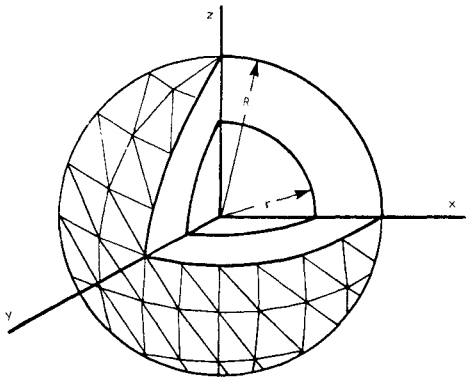

Fig. 2 Gridwork discretization details for a sphere; doublets located on the surface of inner sphere of radius r.

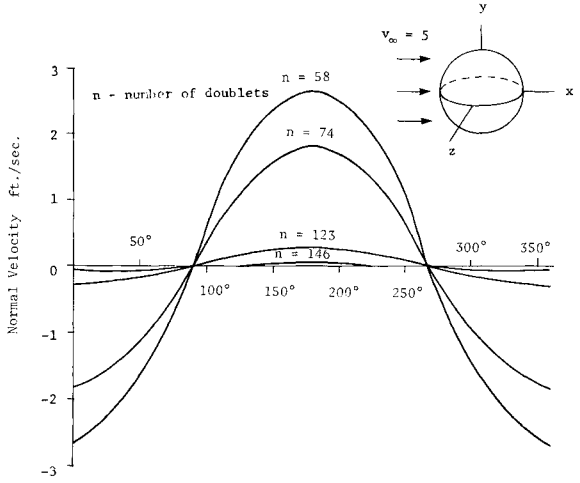

Fig. 3 Normal velocity variation on the outer surface of the sphere along the x-z plane.

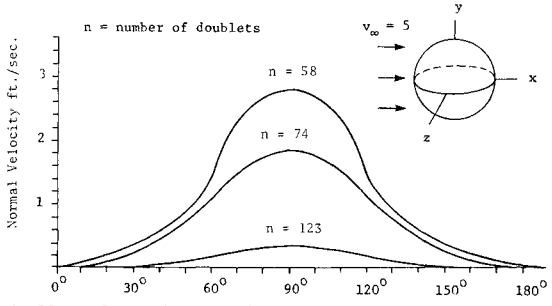

Fig. 4 Normal velocity variation on the outer surface of the sphere along the x-y plane.

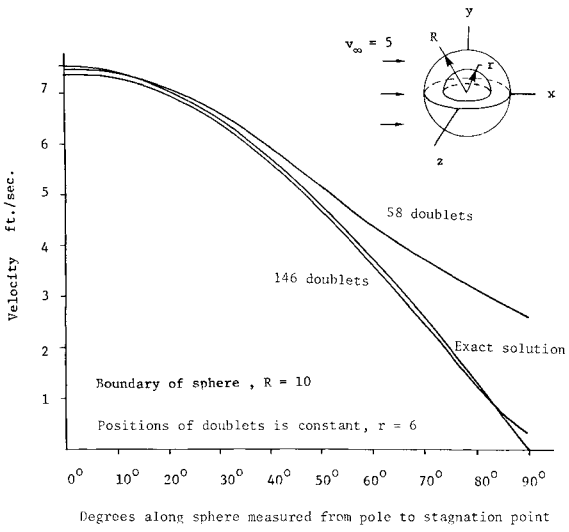

Fig. 5 Variation of the magnitude of velocity alone x-z plane as doublet positions are changed (number of doublets remaining constant).

Table 1 Position coordinates for 23 doublets

Doublet	Coordinates of doublet positions (ft)		
	x	y	z
1	-3.90	-6.70	8.60
2	-4.00	-6.10	-8.40
3	-3.80	0.25	-14.50
4	-1.60	0.86	13.70
5	20.60	1.40	14.00
6	17.10	-1.50	3.40
7	10.80	0.26	-6.80
8	19.10	-2.50	-4.90
9	18.60	-1.80	-5.20
10	22.20	-6.90	-0.06
11	0.87	1.20	--11.60
12	9.90	-6.90	0.00
13	18.10	-5.20	0.08
14	23.20	-4.70	1.80
15	-1.90	-3.40	-5.10
16	2.00	-0.79	8.80
17	9.30	0.80	7.30
18	-0.20	-7.30	-3.10
19	4.90	-3.30	1.50
20	-0.12	-7.50	3.30
21	27.70	-0.34	0.10
22	18.60	-3.40	2.50
23	4.30	-0.71	-7.30

curate results with few doublets, whereas a poorly arranged initial location will require many more doublets for an accurate solution.

The second example is the analysis of the flow around the USSC Mackinaw. The bow of the ship is modeled by a series of doublets placed inside the bow, see the table for their coordinates. The axes of the doublets where chosen parallel to the flow as shown in Fig. 7. The variation of the error function Γ^* as the positions of the doublets are varied is plotted in Fig. 8. Thus, the optimization procedure produced the configuration of doublets shown in Fig. 7. From a set of results three-dimensional computer drawn streamlines have also been produced. It was possible to keep the number of equations to be solved to a minimum. From the analysis of other boundary conditions such as for a pitching motion of the ship, the optimization procedure was proven to be also efficient.

Incremental changes in the boundary conditions did not produce large changes in the positions of the doublets any more. The potential flow around the bow of the ship, as indicated in Fig. 7, was analyzed using 23 doublets, and it required the solution of only 23 equations.

Previous numerical methods developed for the analysis of potential flow, using a set of sources distributed on the surface of the body, determined the vortex configuration based on either experience or intuition. The numerical technique presented in this paper gives a satisfactory solution to this problem by finding the optimum configuration of the set of sources.

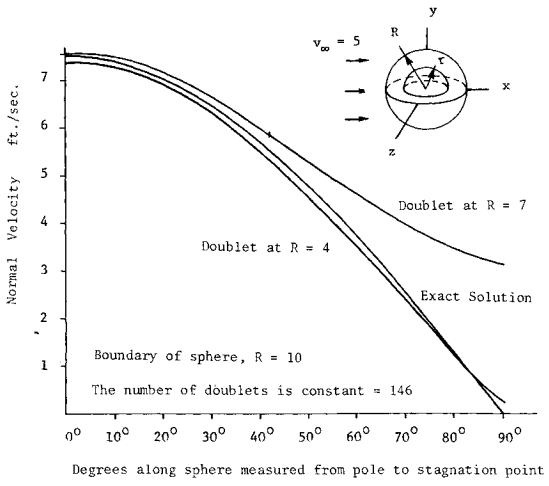

Fig. 6 Variation of the magnitude of the velocity alone x-z plane as the number of doublets is changed (the position of the doublets remains constant).

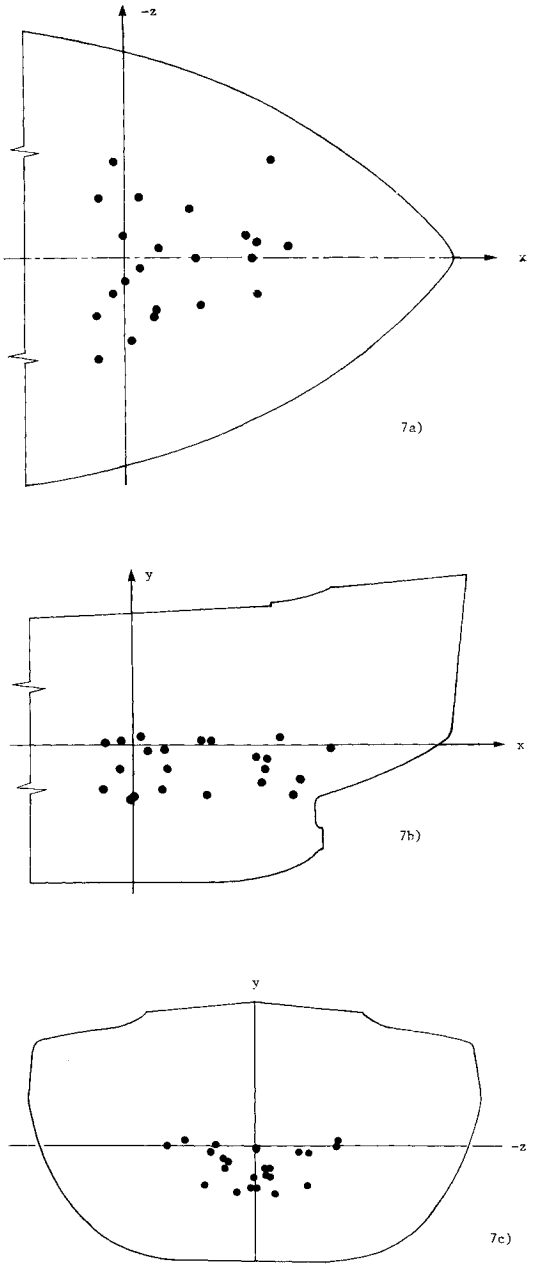

Fig. 7 Configuration of doublets inside ship hull.

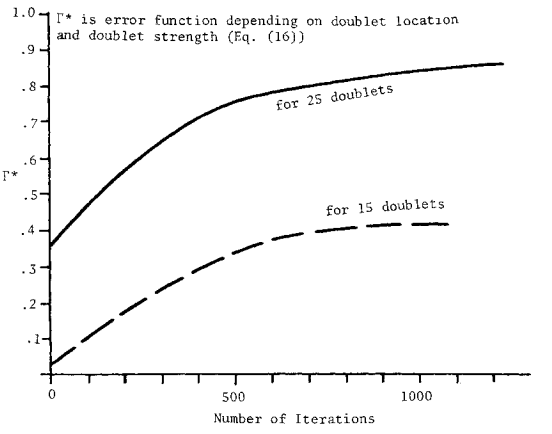

Fig. 8 Variation of the error function with the number of iterations in the optimization procedure.

Appendix A

Proof for Eqs. (13) and (14)

By defining

$$\tilde{S}=D^{1/2}S \tag{A1}$$

and

$$\tilde{A}=D^{1/2}A \tag{A2}$$

Eq. (12) becomes

$$\Gamma=\frac{\tilde{S}^t\tilde{A}(\tilde{A}^t\tilde{A})^{-1}\tilde{A}^t\tilde{S}}{\tilde{S}^t\tilde{S}} \tag{A3}$$

Since the product A^tA is a symmetric positive-definite matrix it can be written in terms of its eigenvalues and eigenvectors as follows

$$\tilde{A}^t\tilde{A}=\sum_{i=1}^{n}\lambda_i p_i p_i^t \tag{A4}$$

and

$$(\tilde{A}^t\tilde{A})^{-1}=\sum_{i=1}^{n}\frac{1}{\lambda_i}p_i p_i^t \tag{A5}$$

By defining also a vector q_i where

$$q_i=\tilde{A}p_i \tag{A6}$$

Eq. (A3) can be written as

$$\Gamma=(\tilde{S}^t\Big[\sum_{i=1}^{n}\frac{q_i q_i^t}{\lambda_i}\Big]\tilde{S}/\tilde{S}^t\tilde{S}) \tag{A7}$$

Since S^* is a vector of order $(mx1)$ it can be written as

$$S^*=\sum_{i=1}^{n}\beta_i q_i+\epsilon \tag{A8}$$

where

$$\epsilon^t q_i=0 \tag{A9}$$

Also from Eqs. (A5) and (A6) one can show that,

$$q_i^t q_i=\lambda_i \tag{A10}$$

Substituting Eq. (A8) and using Eq. (A9), Eq. (A7) becomes

$$\Gamma = \frac{\sum_{i=1}^{n} \lambda_i \beta_i^2}{\left[\sum_{i=1}^{n} \lambda_i \beta_i^2\right] + \epsilon^t \epsilon} \leq 1 \tag{A11}$$

From Eqs. (A8) and (A11) one can observe the validity of Eqs. (13) and (14).

Proof for Eq. (16)

The inequality in Eq. (16) is satisfied when

$$[Q^t(\tilde{A}^t\tilde{A})^{-1}Q][Q^t(\tilde{A}^t\tilde{A})Q] \geq (Q^tQ)^2 \tag{A12}$$

where

$$Q = A^tDS = \tilde{A}^t\tilde{S} \tag{A13}$$

A representation of vector Q in terms of the eigenvectors p_i will give

$$Q = \sum_{i=1}^{n} \alpha_i p_i \tag{A14}$$

Using Eqs. (A4) and (A5), one can write,

$$Q^t(\tilde{A}^t\tilde{A})Q = \sum_{i=1}^{n} \lambda_i \alpha_i^2 \tag{A15}$$

$$Q^t(\tilde{A}^t\tilde{A})^{-1}Q = \sum_{i=1}^{n} \frac{\alpha_i^2}{\lambda_i} \tag{A16}$$

and

$$Q^tQ = \sum_{i=1}^{n} \alpha_i^2 \tag{A17}$$

The inequality of Eq. (A12) can then be written as

$$\left[\sum_{i=1}^{n} \lambda_i \alpha_i^2\right]\left[\sum_{j=1}^{n} \frac{\alpha_j^2}{\lambda_j}\right] \geq \left[\sum_{i=1}^{n} \alpha_i^2\right]\left[\sum_{j=1}^{n} \alpha_j^2\right] \tag{A18}$$

or

$$\sum_{i=1}^{n} \sum_{j=1}^{n} \left(\frac{\lambda_i}{\lambda_j} - 1\right)\alpha_i^2\alpha_j^2 \geq 0 \tag{A19}$$

Expanding the expression in Eq. (A19) one can show that this inequality is valid when

$$\frac{\lambda_i}{\lambda_j} + \frac{\lambda_j}{\lambda_i} - 2 \geq 0 \tag{A20}$$

Equation (A20) becomes an equality when $i \neq j$. However, for $i=j$, and $\lambda_i, \lambda_j > 0$ and since $(\tilde{A}^t\tilde{A})$ is a positive-definite matrix, the inequality in Eq. (A19) is valid.

References

[1] Hess, J. L. and Smith, A. M. O., "Calculation of Potential Flow About Arbitrary Bodies," *Progress in Aerospace Sciences*, Vol. 8, edited by D. Kuchemann, Pergamon Press, New York, 1967, pp. 1-138.

[2] Hess, J. L., "Calculation of Potential Flow About Arbitrary Three-Dimensional Lifting Bodies," Rept. MDC-J5679-01, Oct. 1972, Douglas Aircraft Co., Long Beach, Calif.

[3] Argyris, J. H. Scharpf, D. W., "Two and Three-Dimensional Potential Flow by the Method of Singularities," *Aeronautical Journal*, Royal Aeronautical Society, Vol. 73, Nov. 1969, pp. 959-961.

[4] Kress, R., "Treatment of the Prager Problem of Potential Theory by the Integral Equation Method," *High-Speed Computing in Fluid Dynamics – The Physics of Fluids Supplement II*, Vol. 12, Dec. 1969, pp. 120-125.

[5] Morino, L. and Kuo, C. C., "Subsonic Potential Aerodynamics for Complex Configurations: A General Theory," *AIAA Journal*, Vol. 12, Feb. 1974, pp. 191-197.

[6] Prager, W., "Die Druckverteilung an Koerpern in ebener Potentialstroemung," *Zeitschrift fuer Physik*, Vol. XXIX, 1928, pp. 865-869.

[7] von Karman, "Berechnung der Druckverteilung an Luftschiffkoerpern," *Abhandlungen aus dem Aerodynamischen Institut an der Technischen Hochschule*, Aachen, Heft 6, 1927, pp. 1-17.